Distinguishing between pre- and post-incision under general anesthesia by spectral and recurrence analysis of EEG data

Mariia Fedotenkova, Axel Hutt, Peter Beim Graben, James W. Sleigh

Distinguishing between pre- and post-incision under general anaesthesia by spectral and recurrence analysis of EEG data

Mariia Fedotenkova[1] • Axel Hutt[1] • Peter beim Graben[1,2] • James W. Sleigh[3]

[1] NEUROSYS Team, INRIA CR Nancy - Grand Est, Loria, CNRS, Université de Lorraine, Villers-les-Nancy, 54600, France
[2] Bernstein Center for Computational Neuroscience, Berlin, Germany
[3] Department of Anesthesia, Waikato Clinical School of the University of Auckland, Hamilton 3206, New Zealand

E-mail: mariia.fedotenkova@inria.fr

Motivation

- Nowadays, surgical operations are impossible to imagine without general anesthesia, which involves loss of consciousness, immobility, amnesia and analgesia. Understanding mechanisms underlying each of these effects guarantees well-controlled medical treatment. Current work focuses on analgesia effect of general anesthesia, more specifically, on patients reaction on nociception stimuli. We study EEG data from patients undergoing surgery, focusing on two states: pre-incision and post-incision.

- Data:
  - Single-electrode EEG recordings from surgical operations.
  - 115 patients.
  - 30-second long signals from pre- and post-incision.
  - Anesthetics: propofol & desflurane.
  - Some of the patients reported on having dreams.

- Analysis:
  - Power spectral analysis: Welch PSD estimate, regression fitting.
  - Time-frequency analysis: methods of conventional and reassigned spectrogram, continuous wavelet transform.
  - Use average power in EEG bands obtained from TFRs as multidimensional signal.
  - Recurrence analysis: visualization of structural patterns in multidimensional signals, data-driven estimation of optimal ε parameter by symbolic dynamics
  - Supervised classification: linear discriminant analysis, support vector machine

Power spectral analysis

Power spectral density (PSD) estimates were obtained with Welch's method. We are particularly interested in power in α- and δ-bands. Changes in band power between pre- and post-incisional states should be estimated relatively to the power of brain background activity. It is well known that EEG power spectrum decays with higher frequencies according to the following law [1]:

$$P(f) \sim \frac{a}{f^b}$$

Such behavior might be attributed to background activity. We here propose deviation from this model by using Lorentzian curve:

$$P_{fit}(f) = \frac{a}{f^b + c}$$

Features extracted from power spectral analysis: total power, power in α- and δ-bands, coefficients a, b, and c of fitted Loretzian curvep.

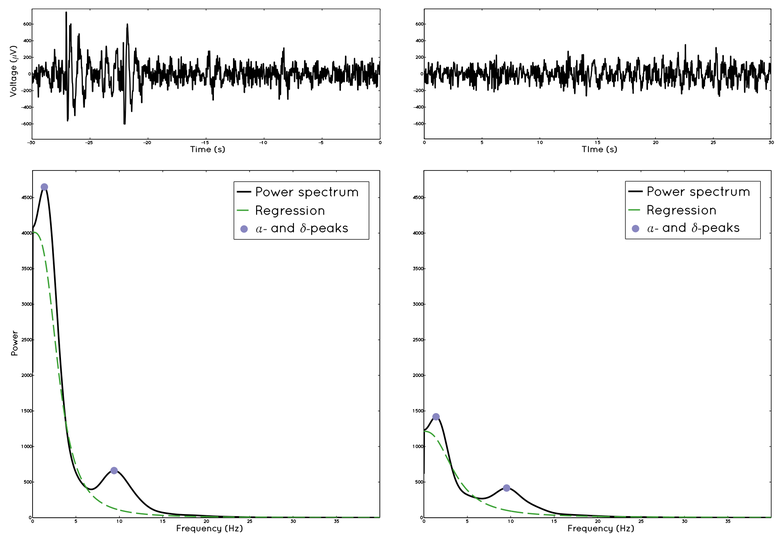

Fig. 1: EEG signals (top) and their corresponding PSD estimates (bottom) for two states: 30 s before the incision (left) and 30 s after the incision (right) for one patient.

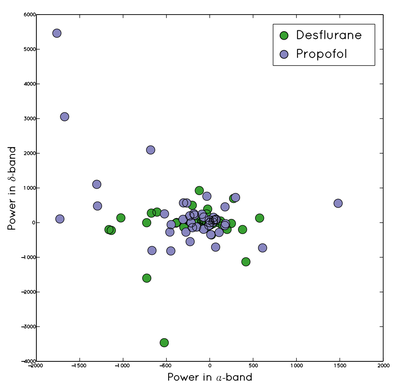

Fig. 2: Changes in average power between pre- and post-incision in δ-band versus changes in α- band

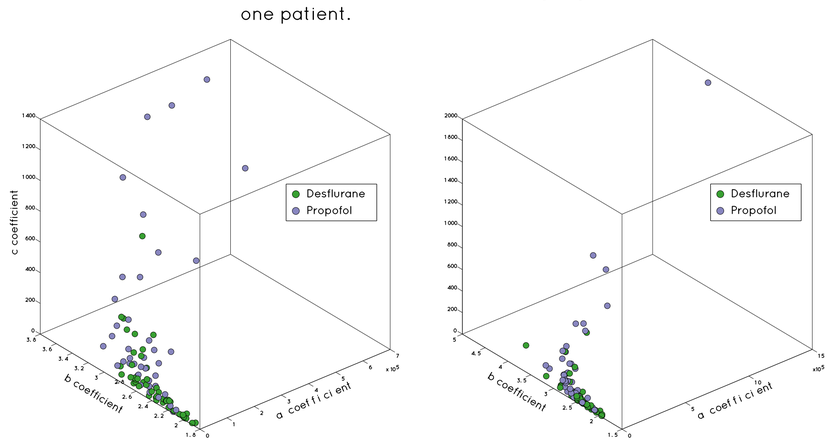

Fig. 3: Joint distribution of background activity model's parameters, results for pre-incision (left) and post-incision (right).

Time-frequency analysis

Time-frequency analysis expands power spectral analysis to non stationary signals. Here, three time-frequency representations were used: continuous wavelet transform [2], conventional and reassigned spectrograms [3]. Another purpose of this analysis is to perform reconstruction of multi-dimensional signal from single time series for further use in recurrence analysis.

Continuous wavelet transform

$$WT_x(a,\tau) = \langle x(t), \psi_{a,\tau} \rangle = \frac{1}{\sqrt{a}} \int_{-\infty}^{+\infty} x(\tau) \psi^* \left(\frac{t-\tau}{a} \right) dt$$

Conventional spectrogram

$$S_x^g(t,f) = |STFT(t,f)|^2 = \left| \int_{-\infty}^{+\infty} x(\tau) g^*(\tau - t) e^{-i2\pi f \tau} d\tau \right|$$

Reassigned spectrogram

$$\hat{S}_x^g(t,f) = \iint_{-\infty}^{+\infty} S_x^g(\tau,\xi) \delta(f - \hat{f}(x;\tau,\xi)) \delta(t - \hat{t}(x;\tau,\xi)) d\tau d\xi$$

$$\hat{t}(x;t,f) = \frac{\iint_{-\infty}^{+\infty} \tau W_h(t-\tau, f-\xi) W_x(\tau,\xi) d\tau d\xi}{\iint_{-\infty}^{+\infty} W_h(t-\tau, f-\xi) W_x(\tau,\xi) d\tau d\xi}$$

$$\hat{f}(x;t,f) = \frac{\iint_{-\infty}^{+\infty} \xi W_h(t-\tau, f-\xi) W_x(\tau,\xi) d\tau d\xi}{\iint_{-\infty}^{+\infty} W_h(t-\tau, f-\xi) W_x(\tau,\xi) d\tau d\xi}$$

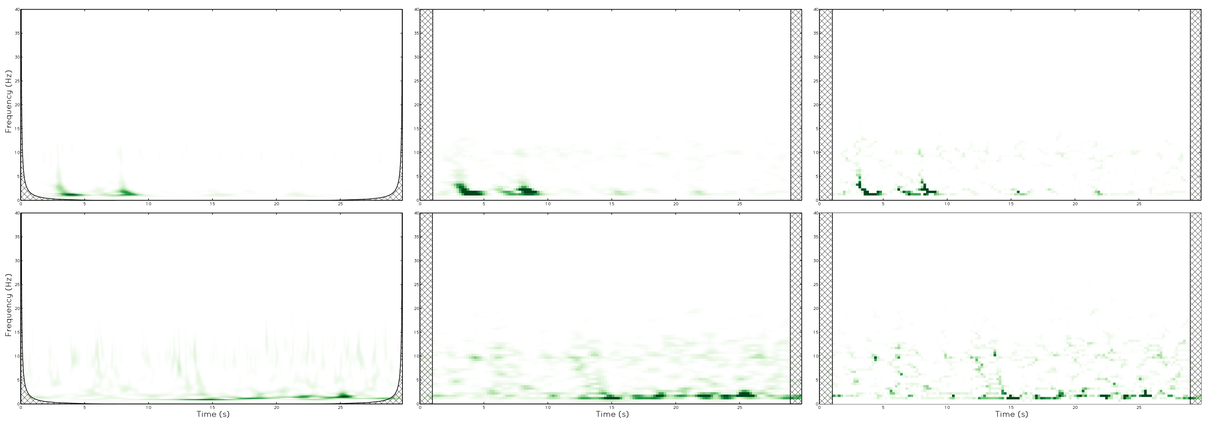

Fig. 4: Time-frequency representations for EEG data shown in Fig.1. Top row is pre-incision, bottom row is post-incision. Time-frequency representations are: continuous wavelet transform (left), spectrogram (middle) and reassigned spectrogram (right).

Recurrence analysis

Recurrence analysis allows to visualize dynamics of multidimensional variables with 2D recurrence plots [4]. At this step original time series is re-written as symbolic sequence using recurrence matrix as rewriting grammar. It also used to estimate optimal value of ε parameter by maximizing utility function computed from a resulting symbolic sequence [5]. As a utility function Shannon entropy is used here, the development of new, more structure-oriented criteria is work in progress. This step of the analysis provided us with three features for future classification: entropy, symbolic repertoire and Lempel-Ziv complexity [6].

Recurrence plot

$$R_{ij} = \Theta\left(\varepsilon - ||x_j - x_i||\right),$$
$$x_i \in \mathbb{R}^d$$

Shannon entropy

$$H(\varepsilon) = -\sum_{k=1}^{M(\varepsilon)} p_k \log p_k$$

Lempel-Ziv complexity

$$\lim_{n\to\infty} c_\varepsilon(n) = \frac{n}{\log_{M(\varepsilon)}(n)}$$

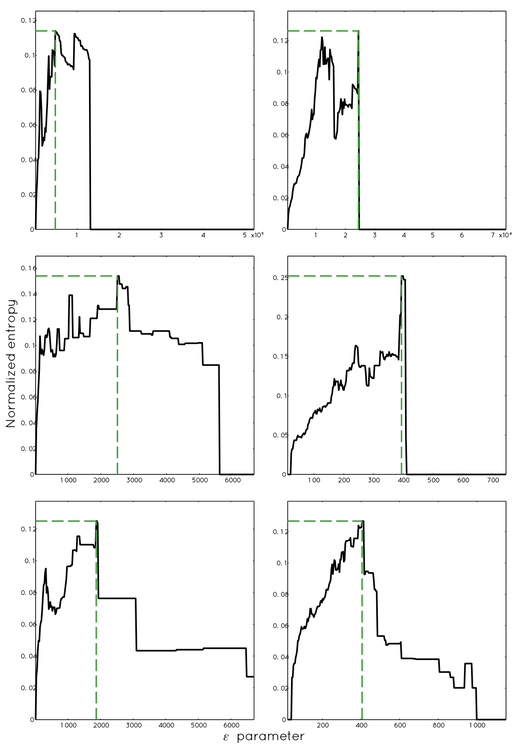

Fig. 5: Distribution of entropy obtained from recurrence plots over ε parameter for EED data from Fig.1. Here, pre-incision (left) and post-incision (right). Recurrence plots were calculated for power bands computed from time-frequency representations as in Fig.4: wavelet transform (top), spectrogram (middle) and reassigned spectrogram (bottom).

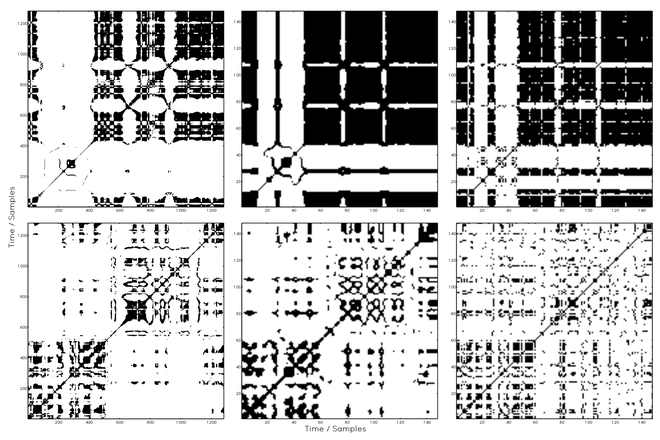

Fig. 6: Recurrence plots with optimal ε as shown in Fig.5 for EED data from Fig.1. Here, pre-incision (top) and post-incision (bottom). Recurrence plots were calculated for power bands computed from time-frequency representations as in Fig.4: wavelet transform (left), spectrogram (right) and reassigned spectrogram (right).

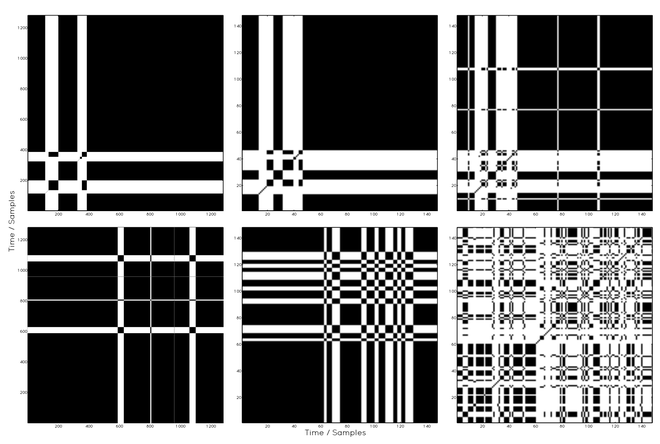

Fig. 7: Same as Fig.6 but recurrence plots obtained from symbolic sequence obtained with optimal ε parameter.

References

1. Bédard, C. & Destexhe, A. Macroscopic Models of Local Field Potentials and the Apparent 1/f Noise in Brain Activity. Biophysical Journal 96, 2589–2603 (2009).
2. Jordan, D., Miksad, R. W. & Powers, E. J. Implementation of the continuous wavelet transform for digital time series analysis. Review of Scientific Instruments 68, 1484 (1997).
3. Auger, F. et al. Time-Frequency Reassignment and Synchrosqueezing: An Overview. IEEE Signal Processing Magazine 30, 32–41 (2013).
4. Marwan, N., Carmenromano, M., Thiel, M. & Kurths, J. Recurrence plots for the analysis of complex systems. Physics Reports 438, 237–329 (2007).
5. Graben, P. B. & Hutt, A. Detecting event-related recurrences by symbolic analysis: applications to human language processing. Philos Trans A Math Phys Eng Sci 373, (2015).
6. Lempel, A. & Ziv, J. On the Complexity of Finite Sequences. IEEE Transactions on Information Theory 22, 75–81 (1976).